## Supplementary information

# Engineering tumor-specific gene nanomedicine to recruit and activate T cells for enhanced immunotherapy

Yue Wang[#,1], Shi-Kun Zhou[#,1], Yan Wang[2], Zi-Dong Lu[2], Yue Zhang[1,3], Cong-Fei Xu*[,1,3,4], Jun Wang*[,1,3,5]

[1]School of Biomedical Sciences and Engineering, South China University of Technology, Guangzhou International Campus, Guangzhou 511442, P.R. China

[2]School of Medicine, South China University of Technology, Guangzhou 510006, P.R. China

[3]National Engineering Research Center for Tissue Restoration and Reconstruction, South China University of Technology, Guangzhou 510006, P.R. China

[4]Guangdong Provincial Key Laboratory of Biomedical Engineering, South China University of Technology, Guangzhou 510006, P.R. China

[5]Key Laboratory of Biomedical Materials and Engineering of the Ministry of Education, South China University of Technology, Guangzhou 510006, P.R. China

[#]Yue Wang and Shi-Kun Zhou contributed equally to this work.

***Corresponding author:** Cong-Fei Xu, xucf@scut.edu.cn, Jun Wang, mcjwang@scut.edu.cn

**Content**

Supplementary Fig. 13 Percentages of $CD3^+$ T cells in melanoma after different treatments.

Supplementary Fig. 14 Percentages of granzyme $B^+$, $perforin^+$, IFN-$\gamma^+$ T cells in melanoma after different treatments.

Supplementary Fig. 15 Percentages of $CD3^+$ T cells in melanoma after $NP_{Sur\text{-}C9AP}$ treatment.

Supplementary Fig. 16 Percentages of $CD3^+$ T cells in CT26, Panc02 and 4T1 tumors after $NP_{Sur\text{-}C9AP}$ treatment.

Supplementary Fig. 17 Percentages of NK cells in CT26, Panc02 and 4T1 tumors after $NP_{Sur\text{-}C9AP}$ treatment.

Supplementary Table. 1 Primer sequences of qRT-PCR analysis.

Supplementary Table. 2 Sequences of Tyrosinase (Tyr) promoter and Survivin (Sur) promoter.

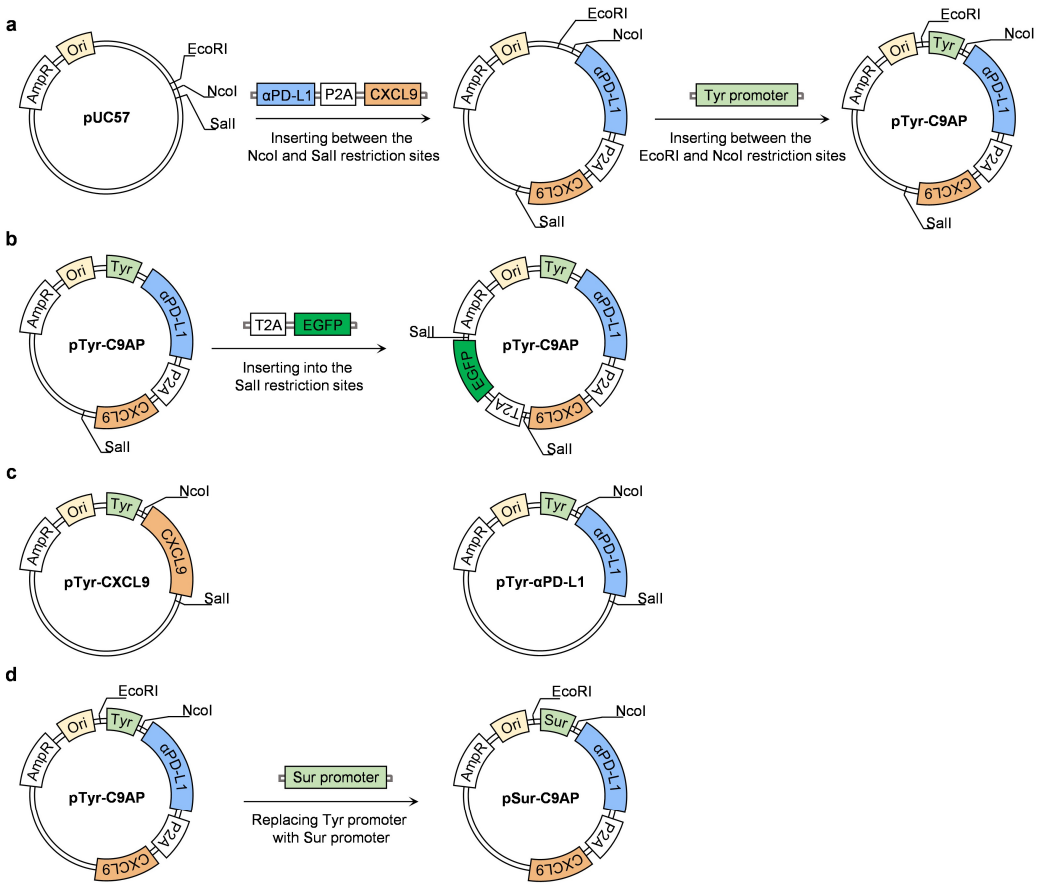


**Supplementary Fig. 1 Construction of pTyr-C9AP, pSur-C9AP and other control plasmids. a** Construction of pTyr-C9AP by inserting αPD-L1-P2A-CXCL9 fragment and Tyr promoter into pUC57 backbone plasmid. pTyr-C9AP was used to co-express CXCL9 and αPD-L1 specifically in melanoma cells. **b** Construction of pTyr-C9AP containing EGFP reporter gene by inserting T2A-EGFP fragment into SalI site. pTyr-C9AP containing EGFP reporter gene was used to analyze the melanoma-specificity of $NP_{Tyr\text{-}C9AP}$. **c** Maps of pTyr-CXCL9 and pTyr-αPD-L1, which specifically express CXCL9 or αPD-L1 alone in melanoma cells, were used as the controls of pTyr-C9AP. **d** Construction of pSur-C9AP by replacing the Tyr promoter of pTyr-C9AP with Sur promoter. pSur-C9AP was used to co-express CXCL9 and αPD-L1 specifically in different tumor cells.

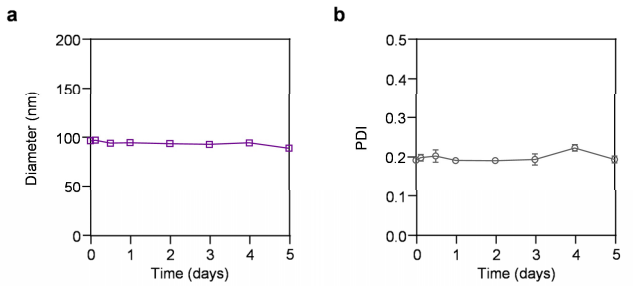


**Supplementary Fig. 2 Stability test of $NP_{Tyr\text{-}C9AP}$.** **a**, **b** Diameter (**a**) and polydispersity index (PDI) (**b**) of $NP_{Tyr\text{-}C9AP}$ after being incubated in DMEM medium containing 10% FBS. The diameter and PDI were detected by Zetasizer Nano ZS90 at different time periods. The data are shown as the means ± SEM of n = 3.

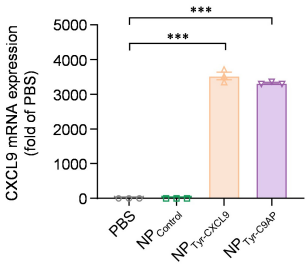


**Supplementary Fig. 3 mRNA expression of CXCL9 in $NP_{Tyr\text{-}C9AP}$-transfected B16-F10 cells.** B16-F10 cells were incubated with PBS, $NP_{Control}$, $NP_{Tyr\text{-}CXCL9}$ or $NP_{Tyr\text{-}C9AP}$ for 6 h, and CXCL9 mRNA expression was detected by qRT-PCR at 48 h after different transfections. The data are shown as the means ± SEM of n = 3. One-way ANOVA with Tukey's multiple comparison test. ***$P$<0.001.

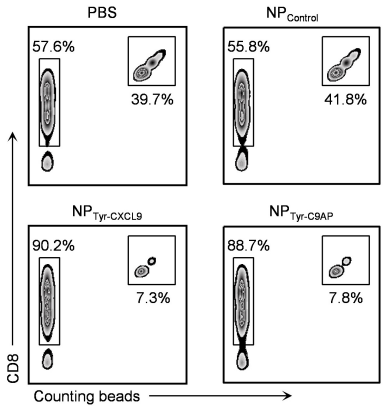


**Supplementary Fig. 4 Representative flow cytometry plots of CD8$^+$ T cells recruited into the lower chamber of the transwell plates.** Activated CD8$^+$ T cells were labeled with DiI dye, and were cultured in the upper chamber of transwell plates at the density of $1\times10^6$ cells per well. Then, the culture supernatants of PBS, $NP_{Control}$, $NP_{Tyr\text{-}CXCL9}$ or $NP_{Tyr\text{-}C9AP}$-transfected B16-F10 cells were placed in the lower chamber. Three hours after incubation, CD8$^+$ T cells recruited in the lower chamber were collected and were labeled with FITC anti-mouse CD8a antibody. Then, 10 μl of Precision Count Beads were added into each sample before being analyzed by flow cytometry. The numbers of recruited CD8$^+$ T cells were calculated using the formula: Absolute Count of CD8$^+$ T Cells = Ratio of CD8$^+$ T Cells/Counting Beads × Absolute Count of Counting Beads.

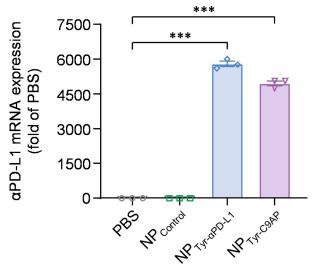


**Supplementary Fig. 5 mRNA expression of αPD-L1 in $NP_{Tyr\text{-}C9AP}$-transfected B16-F10 cells.** B16-F10 cells were incubated with PBS, $NP_{Control}$, $NP_{Tyr\text{-}\alpha PD\text{-}L1}$ or $NP_{Tyr\text{-}C9AP}$ for 6 h, and αPD-L1 mRNA expression was detected by qRT-PCR at 48 h after different transfections. The data are shown as the means ± SEM of n = 3. One-way ANOVA with Tukey's multiple comparison test. ***$P$<0.001.

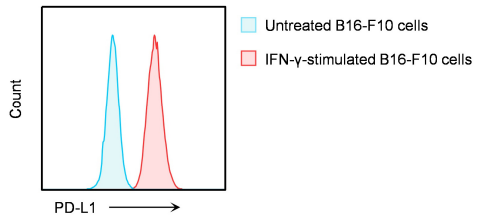


**Supplementary Fig. 6 Representative flow cytometry plots of PD-L1 expression of IFN-γ-stimulated-B16-F10 cells.** B16-F10 cells were stimulated with IFN-γ (20 ng $ml^{-1}$) for 48 h. Then, the IFN-γ-stimulated B16-F10 cells were stained with PE anti-mouse PD-L1 antibody (clone: 10F.9G2, BioLegend), and the expression of PD-L1 was analyzed by flow cytometry. The data are representative of three independent experiments

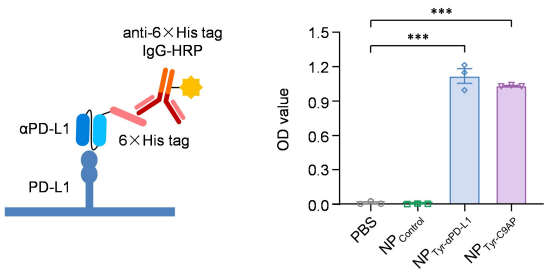


**Supplementary Fig. 7 ELISA analysis of the capability of αPD-L1 to bind PD-L1.**

The culture supernatants of B16-F10 cells transfected with PBS, $NP_{Control}$, $NP_{Tyr\text{-}\alpha PD\text{-}L1}$ or $NP_{Tyr\text{-}C9AP}$ were collected at 72 h after different transfections. Then, the culture supernatants were added into the ELISA plates coated with PD-L1 molecule (SinoBiological, Beijing, China). One hour after incubation, the quantity of αPD-L1 that bound to PD-L1 molecule was detected using anti-6×His tag IgG-HRP (SinoBiological) to label 6×His tag of αPD-L1. The data are shown as the means ± SEM of n = 3. One-way ANOVA with Tukey's multiple comparison test. ***$P$<0.001.

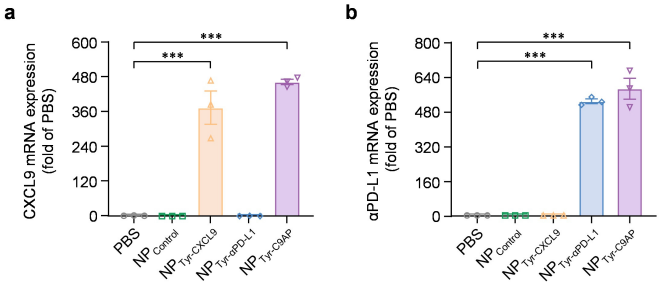


**Supplementary Fig. 8 mRNA expression of CXCL9 (a) and αPD-L1 (b) in melanoma after different treatments.** Mice bearing B16-F10 melanoma were intravenously injected with PBS, $NP_{Control}$, $NP_{Tyr\text{-}CXCL9}$, $NP_{Tyr\text{-}\alpha PD\text{-}L1}$ or $NP_{Tyr\text{-}C9AP}$ ($n$ = 3 mice per group). Seventy-two hours after injection, the mRNA expression of CXCL9 and αPD-L1 in melanoma tissues were detected by qRT-PCR. The data are shown as the means ± SEM of n = 3. One-way ANOVA with Tukey's multiple comparison test. ***$P$<0.001.

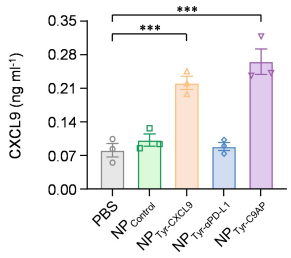


**Supplementary Fig. 9 Serum concentrations of CXCL9 after different treatments.** Mice bearing B16-F10 melanoma were intravenously injected with PBS, $NP_{Control}$, $NP_{Tyr\text{-}CXCL9}$, $NP_{Tyr\text{-}\alpha PD\text{-}L1}$ or $NP_{Tyr\text{-}C9AP}$ ($n$ = 3 mice per group). Seventy-two hours after injection, the serum samples were collected, and the concentrations of CXCL9 in the serum were detected by ELISA. The data are shown as the means ± SEM of n = 3. One-way ANOVA with Tukey's multiple comparison test. ***$P$<0.001.

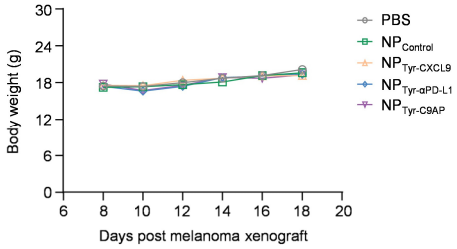


**Supplementary Fig. 10 Body weights of mice bearing B16-F10 melanoma treated with $NP_{Tyr\text{-}C9AP}$ or other controls.** Mice bearing B16-F10 melanoma were intravenously injected with PBS, $NP_{Control}$, $NP_{Tyr\text{-}CXCL9}$, $NP_{Tyr\text{-}\alpha PD\text{-}L1}$ or $NP_{Tyr\text{-}C9AP}$ every other day for five injections (n = 10 mice per group), as illustrated in Fig. 4c. The body weights of the mice were monitored every other day since the first injection. The data are shown as the means ± SEM of n = 10.

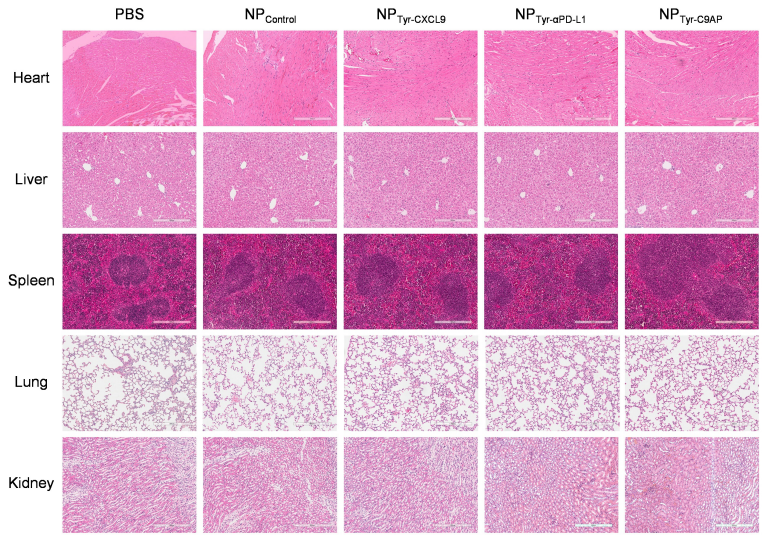


**Supplementary Fig. 11 Representative H&E staining of major organs after different treatments.** The major organs (including heart, liver, spleen, lung and kidney) of mice bearing B16-F10 melanoma were collected at the end of different treatments, and the histopathology of each organ was analyzed by haemotoxylin & eosin (H&E) staining. Scale bar = 300 μm.

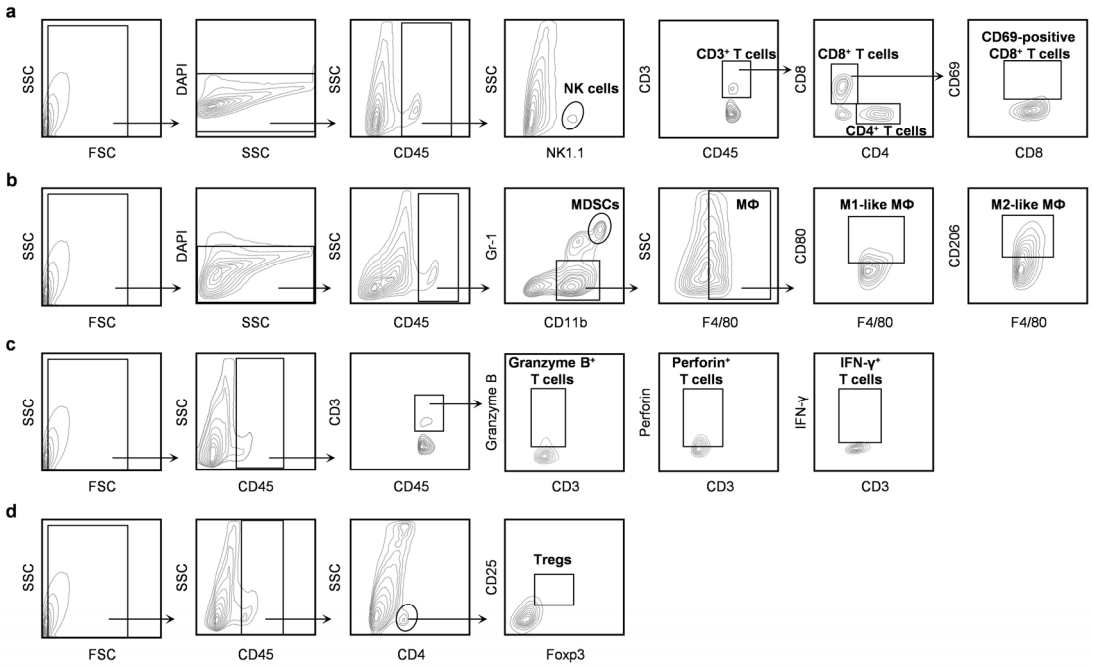


**Supplementary Fig. 12 Gating strategies of flow cytometry analysis of immune cells in melanoma. a** Gating strategies of $CD3^+$, $CD4^+$, $CD8^+$, CD69-positive $CD8^+$ T cells and natural killer (NK) cells. **b** Gating strategies of myeloid-derived suppressor cells (MDSCs), M1-like and M2-like macrophages (MΦ). **c** Gating strategies of granzyme $B^+$, perforin$^+$ and IFN-$\gamma^+$ T cells. **d** Gating strategies of regulatory T cells (Tregs).

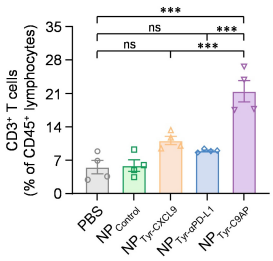


**Supplementary Fig. 13 Percentages of CD3$^+$ T cells in melanoma after different treatments.** The representative flow cytometry plots were correspondingly shown in Fig. 5a. The data are shown as the means ± SEM of n = 4. One-way ANOVA with Tukey's multiple comparison test. ***$P$<0.001; ns indicates no significant difference.

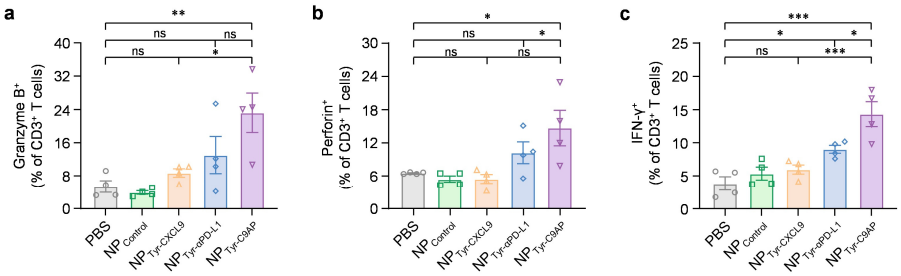


**Supplementary Fig. 14 Percentages of granzyme B$^+$ (a), perforin$^+$ (b), IFN-γ$^+$ (c) T cells in melanoma after different treatments.** The representative flow cytometry plots were correspondingly shown in Fig. 5h. The data are shown as the means ± SEM of n = 4. One-way ANOVA with Tukey's multiple comparison test. **P*<0.05; ***P*<0.01; ****P*<0.001; ns indicates no significant difference.

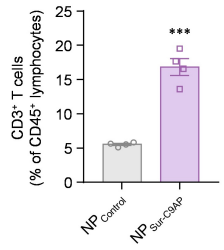


**Supplementary Fig. 15 Percentages of $CD3^+$ T cells in melanoma after $NP_{Sur\text{-}C9AP}$ treatment.** Mice bearing B16-F10 melanoma were intravenously injected with $NP_{Control}$ or $NP_{Sur\text{-}C9AP}$ every other day for five injections. At the end of the treatments, the melanoma tissues were isolated, and the percentages of $CD3^+$ T cells were analyzed by flow cytometry. The representative flow cytometry plots were correspondingly shown in Fig. 6e. The data are shown as the means ± SEM of n = 4. Student's *t*-test. ***$P$<0.001.

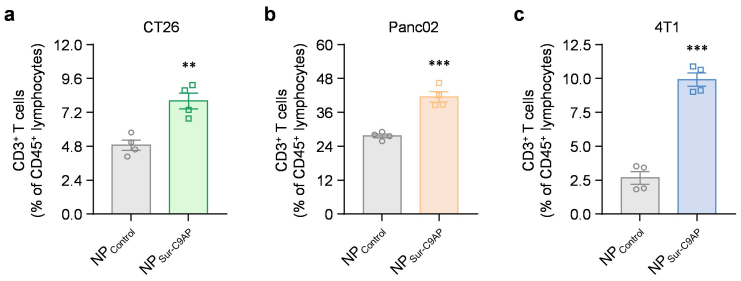


**Supplementary Fig. 16 Percentages of CD3$^+$ T cells in CT26 (a), Panc02 (b) and 4T1 (c) tumors after NP$_{\text{Sur-C9AP}}$ treatment.** Mice bearing CT26, Panc02 and 4T1 tumors were intravenously injected with NP$_{\text{Control}}$ or NP$_{\text{Sur-C9AP}}$ every other day. At the end of the treatments, the tumor tissues were isolated, and the percentages of CD3$^+$ T cells were analyzed by flow cytometry. The representative flow cytometry plots were correspondingly shown in Fig. 6o to q. The data are shown as the means ± SEM of n = 4. Student's *t*-test. ***P*<0.01; ****P*<0.001.

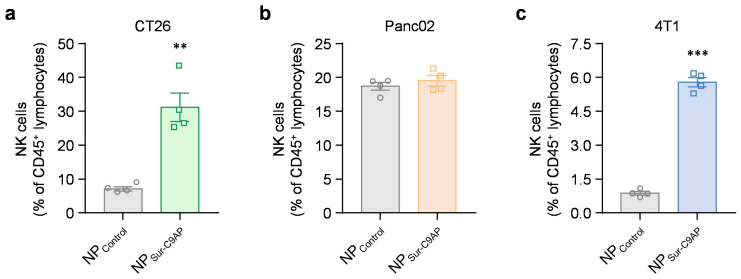


**Supplementary Fig. 17 Percentages of NK cells in CT26 (a), Panc02 (b) and 4T1 (c) tumors after $NP_{Sur\text{-}C9AP}$ treatment.** The data are shown as the means ± SEM of n = 4. Student's *t*-test. ***P*<0.01; ****P*<0.001.

**Supplementary Table. 1 Primer sequences of qRT-PCR analysis.**

| | |
|---|---|
| CXCL9 | Forward: 5’-TCCTCTTGGGCATCATCTTCC-3’<br>Reverse: 5’-TTTGTAGTGGATCGTGCCTCG-3’ |
| αPD-L1 | Forward: 5’-GAATGGGTGGCGTGGATTAG-3’<br>Reverse: 5’-GGCTGTTCATCTGCAGATACG-3’ |
| GAPDH | Forward:5’-AGGTCGGTGTGAACGGATTTG-3’<br>Reverse: 5’-TGTAGACCATGTAGTTGAGGTCA-3’ |

**Supplementary Table. 2 Sequences of Tyrosinase (Tyr) promoter and Survivin (Sur) promoter.**

| | |
|---|---|
| Tyr promoter | 5’-CCTGCAGGTCATAGTTCCTGCCAGCTGACTTTGTCAAGA<br>CAGTGATGTCTGTGTTCCAGCAGTTGTTCTGAGTATCCTTT<br>TCATTATCCACTGTCCTTTCTTCTTAAATTCCACCCCCAACA<br>TTGTAAATAGCTTCTTTCTTAAACTCTGTTCAAAGAACCAG<br>CTTGAGTGTGTCAGCTGCTTCCTGCTGGGGTCCTGGCAAA<br>CCACTAGTGACCTTTATTCATAAGAGATGATGTATTCTTGAT<br>ACTACTTCTCATTTGCAAATTCCAATTATTATTAATTTCATAT<br>CAATTAGAATAATATATCTTCCTTCAATTTAGTTACCTCACTA<br>TGGGCTATGTACAAACTCCAAGAAAAAGTTAGTCATGTGC<br>TTTGCAGAAGATAAAAGCTTAGTGTAAAACAGGCTGAGAG<br>TATTTGATGTAAGAAGGGGAGTGGTTATATAGGTCTTAGCC<br>AAAACATGTGATAGTCACTCCAGGGGTTGCTGGAAAAGAA<br>GTCTGTGACACTCATTAACCTATTGGTGCAGATTTTGTATGA<br>TCTAAAGGAGAC-3’ |
| Sur promoter | 5’-GGCAGGGACGAGCTGGCGCGGCGTCGCTGGGTGCACC<br>GCGACCACGGGCAGAGCCACGCGGCGGGAGGACTACAAC<br>TCCCGGCACACCCCGCGCCGCCCCGCCTCTACTCCCAGAA<br>GGCCGCGGGGGGTGGACCGCCTAAGAGGGCGTGCGCTCC<br>CGACATGCCCCGCGGCGCGCCATTAACCGCCAGATTTGAAT<br>CGCGGGACCCGTTGGCAGAGGTGGCGGCGGCGGCATGGG<br>TGCCCCGACGTTGCCCCCTGCCTGG-3’ |